

# Revisiting Modularity Maximization for Graph Clustering: A Contrastive Learning Perspective

Yunfei Liu\*  
Ant Group  
leo.lyf@antgroup.com

Jintang Li\*†  
Ant Group  
edisonleejt@gmail.com

Yuehe Chen  
Ant Group  
chenyuehe.cyh@antgroup.com

Ruofan Wu  
Ant Group  
wuruofan1989@gmail.com

Ericbk Wang  
Ant Group  
yike.wbk@antgroup.com

Jing Zhou  
Ant Group  
colin.zj@antgroup.com

Sheng Tian  
Ant Group  
tiansheng.ts@antgroup.com

Shuheng Shen  
Ant Group  
shuheng.ssh@antgroup.com

Xing Fu  
Ant Group  
fux008@gmail.com

Changhua Meng  
Ant Group  
changhua.mch@antgroup.com

Weiqiang Wang  
Ant Group  
wang.weiqiang@gmail.com

Liang Chen  
Unaffiliated  
jasonclx@gmail.com

## ABSTRACT

Graph clustering, a fundamental and challenging task in graph mining, aims to classify nodes in a graph into several disjoint clusters. In recent years, graph contrastive learning (GCL) has emerged as a dominant line of research in graph clustering and advances the new state-of-the-art. However, GCL-based methods heavily rely on graph augmentations and contrastive schemes, which may potentially introduce challenges such as semantic drift and scalability issues. Another promising line of research involves the adoption of modularity maximization, a popular and effective measure for community detection, as the guiding principle for clustering tasks. Despite the recent progress, the underlying mechanism of modularity maximization is still not well understood. In this work, we dig into the hidden success of modularity maximization for graph clustering. Our analysis reveals the strong connections between modularity maximization and graph contrastive learning, where positive and negative examples are naturally defined by modularity. In light of our results, we propose a community-aware graph clustering framework, coined MAGI, which leverages modularity maximization as a contrastive pretext task to effectively uncover the underlying information of communities in graphs, while avoiding the problem of semantic drift. Extensive experiments on multiple graph datasets verify the effectiveness of MAGI in terms of scalability and clustering performance compared to state-of-the-art graph clustering methods. Notably, MAGI easily scales a sufficiently large graph with 100M nodes while outperforming strong baselines.

\*Both authors contributed equally to this research.

† Corresponding author.

Permission to make digital or hard copies of part or all of this work for personal or classroom use is granted without fee provided that copies are not made or distributed for profit or commercial advantage and that copies bear this notice and the full citation on the first page. Copyrights for third-party components of this work must be honored. For all other uses, contact the owner/author(s).  
KDD '24, August 25–29, 2024, Barcelona, Spain  
© 2024 Copyright held by the owner/author(s).  
ACM ISBN 979-8-4007-0490-1/24/08.  
<https://doi.org/10.1145/3637528.3671967>

## CCS CONCEPTS

• **Information systems** → *Clustering*; • **Computing methodologies** → *Unsupervised learning*; *Learning latent representations*.

## KEYWORDS

Graph clustering, graph contrastive learning, modularity maximization

### ACM Reference Format:

Yunfei Liu, Jintang Li, Yuehe Chen, Ruofan Wu, Ericbk Wang, Jing Zhou, Sheng Tian, Shuheng Shen, Xing Fu, Changhua Meng, Weiqiang Wang, and Liang Chen. 2024. Revisiting Modularity Maximization for Graph Clustering: A Contrastive Learning Perspective. In *Proceedings of the 30th ACM SIGKDD Conference on Knowledge Discovery and Data Mining (KDD '24)*, August 25–29, 2024, Barcelona, Spain. ACM, New York, NY, USA, 12 pages. <https://doi.org/10.1145/3637528.3671967>

## 1 INTRODUCTION

Graph clustering is a fundamental problem in graph analysis, crucial for uncovering structures and relationships between nodes in a graph. The primary objective of graph clustering is to group or partition the nodes in a graph into clusters or communities based on their structural properties or connectivity patterns. So far, graph clustering has been widely studied and extensively applied across various domains, including social network analysis [28], image segmentation [10] and recommendation systems [26].

As a longstanding field of research, graph clustering continues to evolve through the development of novel algorithms and techniques. Recently, graph neural networks (GNNs) have emerged as the *de facto* deep learning architecture for dealing with graph data [19, 43]. In light of the learning capability of GNNs on graph-structured data, researchers have shifted their attention to exploring GNN-based approaches for graph clustering. Typically, GNNs are employed as encoders to learn node representations, which are often accomplished with an auxiliary task to help uncover the underlying patterns for clustering. As the graph clustering task is commonly approached in

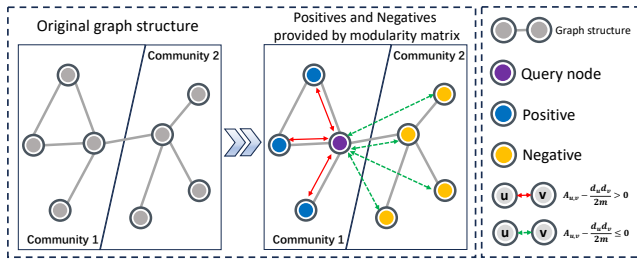


**Figure 1: An illustrative overview of how positive and negative examples of a query node are guided by the “modularity” measure.**

an unsupervised manner due to the absence of labeled annotations, this has motivated the exploration of self-supervised graph learning methods for graph clustering. Contrastive learning [13, 46], which aims to learn representations that bring similar instances closer in the representation space and distances dissimilar ones, has been proven to learn “cluster-preserving” representations [31]. Therefore, recently, graph contrastive learning methods (GCLs) [22, 38, 44, 49] have made significant breakthroughs in graph clustering and gradually become the mainstream approach for graph clustering.

Inspired by [46], early GCLs [44, 51] adopted instance discrimination as a pretext task, aiming to learn representations that are invariant to different augmented views of the graph. Recently, some works have proposed augmentation-free GCLs [9, 20, 24, 48], which extract contrastive information from the graph data itself and construct corresponding pseudo-labels. Several works [20, 24, 48] use K-means [25] and K-Nearest Neighbors (KNN) to mine the potential cluster within graph features, and utilize the clustering results as foundation for positive/negative sample pairs. Although the GCLs mentioned above have achieved significant success in the graph clustering task, we note that these methods still suffer from at least one of the following challenges:

**(C1) Scalability.** Mainstream GCLs typically rely on data augmentation to create multiple views and employ multiple encoders to obtain corresponding representations. However, this poses computational challenges and scalability issues when applied to large-scale graphs. On the other hand, feature-based augmentation-free GCLs require the use of high-cost algorithms such as K-means and KNN to construct pseudo-labels, which also limits their capability to scale to large-scale datasets.

**(C2) Semantic drift.** Pretext tasks play an important role in enabling GCL to better adapt to downstream tasks. A typical approach is to define instance-wise “augmentations” and then pose the problem as that of learning to closely align these augmentations with the original, while keeping them separate from others. However, this type of pretext task neglects the inherent structure of graph data, which can result in semantic drift during downstream clustering tasks [20]. Augmentation-free GCLs can mitigate this by mining the information inherently carried by graph data. However, as previously mentioned, methods based on K-means and KNN lack scalability, and using simple random walks to mine positive samples [9] within a node’s neighborhood can easily lead to a community semantic drift, especially when a node is situated at the edge of a community.

Recently, methods based on neural modularity [27] maximization have made new progress in graph clustering tasks [2, 41]. By using a single GNN encoder to encode the relaxed community assignment matrix, these methods effectively combine the modularity maximization objective with GNNs and achieve state-of-the-art performance in graph clustering tasks. The modularity maximization objective can effectively perceive the potential community structure within networks [23] and provide guidance for representation learning. However, the design of the modularity function is heuristic, and the underlying reasons for its success as an optimization objective remain largely unexplored.

In this work, we provide an in-depth analysis of modularity maximization and bridge the gap between modularity maximization and GCL. Our analysis shows that modularity maximization is essentially graph contrastive learning, where the positive and negative examples are naturally guided by the modularity matrix (see Figure 1). Based on our findings, we attempt to integrate the latest developments in the fields of neural modularity maximization and graph contrastive learning, and propose a community-aware graph clustering framework, coined MAGI. MAGI can mitigate the effects of semantic drift by perceiving the underlying community structures in the graph, and since it doesn’t rely on data augmentation, it can easily scale to a sufficiently large graph with 100M nodes. Our contributions can be summarized as follows:

- **Modularity maximization = contrastive learning.** We establish the connection between modularity maximization and graph contrastive learning. Our findings reveal that modularity maximization can be viewed as leveraging potential community information in graphs for contrastive learning.
- **Community-aware pretext task and scalable framework.** We propose MAGI, a community-aware graph contrastive learning framework that uses *modularity maximization* as its pretext task. MAGI avoids semantic drift by leveraging underlying community structures and eliminates the need for graph augmentation. MAGI incorporates a two-stage random walk approach to perform modularity maximization pretext tasks in mini-batch form, thereby achieving good scalability.
- **Experimental results.** We conduct extensive experiments on 8 real-world graph datasets with different scales. MAGI has consistently outperformed several state-of-the-arts in the task of graph clustering. Notably, MAGI easily scales to an industrial-scale graph with 100M nodes, showcasing its scalability and effectiveness in large-scale scenarios.

## 2 RELATED WORK

### 2.1 Graph clustering

Graph clustering is a widely studied problem in academia and industry. Classical clustering methods involve either solving an optimization problem or using some heuristic, non-parametric approaches. Prominent examples include K-means [25], spectral clustering [35], and Louvain [3]. However, the shallow architecture of these methods limits their performance. With the rise of deep neural networks in graph representation learning, random walk-based methods such as DeepWalk [32] and Node2vec [12] have also been introduced for addressing clustering tasks.

Early works typically focus on single dimension form graphs, e.g., graph structure or node attributes. Thanks to the great ability of graph neural networks (GNNs) [19, 43] in learning jointly structure and attribute information, graph autoencoders stand out as an emerging approach for unsupervised graph learning tasks. For example, GAE and VGAE [18] learn to reconstruct the graph structure as the self-supervised learning task using GNNs. Follow-up works extend GAE by employing Laplacian sharpening [30], Laplacian smoothing [8], generative adversarial learning [29], and masked autoencoding [21]. However, self-supervised learning tasks or pretext tasks in GAEs are not aligned with downstream tasks such as graph clustering. As a result, the learned representations may not effectively capture the relevant information for clustering tasks.

## 2.2 Graph contrastive learning

Over the past few years, graph contrastive learning (GCL) has emerged as a powerful technique for learning representations of graph-structured data. Deep Graph Infomax (DGI) [44] follows the approach of mutual information-based learning, as proposed by adapted [16]. GRACE [51] maximizes the agreement of node representations between two corrupted views of a graph. GraphCL [49] incorporates four graph augmentation techniques to learn unsupervised graph representations through a unified contrastive learning framework. One step further, MVGRL [15] introduces node diffusion and contrasts node-level embeddings with representations of augmented graphs. Following the BYOL [11], BGRL [39] eliminates the need for negative sampling by minimizing an invariance-based loss for augmented graphs within a batch. In light of the success of GCL, there have been attempts to apply GCL techniques to graph clustering and achieve promising results [9, 20, 24, 48]. However, most methods employ classical instance discrimination as the pretext task, which requires sophisticated graph augmentation techniques to obtain meaningful view representations. As a result, they may suffer from challenges such as semantic drift and limitations in scaling up to handle large graphs.

## 2.3 Neural modularity maximization

As one of the most commonly used metrics for community detection, modularity measures the quality of a partition in a network by evaluating the density of connections within communities compared to random connections [27]. Maximizing the modularity directly is proven to be NP-hard [4]. As a result, heuristics such as spectral relaxation [28] and greedy algorithms [3] have been developed to approximate the modularity and find suboptimal but reasonable community partitions. However, previous works focus simply on the graph structure, while ignoring the abundant information associated with the nodes (e.g., attributes). With the advent of graph neural networks, combining them with modularity maximization has become a promising research direction. [1, 47] utilizes an autoencoder to encode the community assignment matrix and combines it with a reconstruction loss to train the autoencoder. [23, 36] and [7, 33, 50] extend this idea by employing (variational) graph autoencoders. [23] explored the benefits brought by high-order proximity and used high-order polynomials of the adjacency

matrix to calculate the high-order modularity matrix. [37] constructs two loss functions based on modularity, corresponding to single and multi-attribute networks, while DMoN [41] introduces collapse regularization to prevent the community allocation matrix from falling into spurious local minima. Despite the recent progress, the underlying mechanism of neural modularity maximization for graph clustering is still not well understood.

## 3 MOTIVATION

In this section, we first provide basic notations throughout this paper. We then introduce preliminary knowledge for modularity-based learning, which is connected to contrastive learning as our motivation.

### 3.1 Problem statement and notations

Given an attribute graph  $\mathcal{G} = (\mathcal{V}, \mathcal{E}, \mathbf{X})$ , where  $\mathcal{V} = \{v_1, v_2, \dots, v_N\}$  denotes a set of nodes and  $N = |\mathcal{V}|$ ;  $\mathcal{E} \subseteq \mathcal{V} \times \mathcal{V}$  denotes corresponding edges between nodes, where each node  $v \in \mathcal{V}$  is associated with a  $d_h$ -dimensional feature vector  $x_v \in \mathbb{R}^{d_h}$ . Let  $\mathbf{X} \in \mathbb{R}^{N \times d_h}$  denote the node attribute matrix and  $\mathbf{A} \in \mathbb{R}^{N \times N}$  the adjacency matrix, respectively. Given the graph  $\mathcal{G}$  and node attributes  $\mathbf{X}$ , the goal of graph clustering is to partition the nodes set  $\mathcal{V}$  into  $C$  partitions  $\{\mathcal{V}_1, \mathcal{V}_2, \mathcal{V}_3, \dots, \mathcal{V}_C\}$  such that nodes in the same cluster are similar/close to each other in terms of the graph structure as well as in terms of attributes.

### 3.2 Revisiting modularity maximization

Modularity [27] is a measure of the graph structure, which measures the divergence between the intra-community edges from the expected one. Formally, given a graph  $\mathcal{G}$ , the modularity ( $Q$ ) is defined as:

$$Q = \frac{1}{2m} \sum_{i,j} (\mathbf{A}_{i,j} - \frac{d_i d_j}{2m}) \delta(c_i, c_j), \quad (1)$$

where  $d_i = \sum_j \mathbf{A}_{i,j}$  is the degree of node  $v_i$ ,  $m = |\mathcal{E}|$  is the total number of edges in the graph, and  $c_i$  is the community to which node  $v_i$  is assigned.  $\delta(c_i, c_j) = 1$  is an indicator function, i.e.,  $\delta(c_i, c_j) = 1$  if  $c_i = c_j$  and 0 otherwise, suggesting whether nodes  $v_i$  and  $v_j$  belong to the same community. Essentially,  $\mathbf{A}_{i,j}$  and  $\frac{d_i d_j}{2m}$  can be regard as the ‘‘observed’’ and ‘‘expected’’ number of edges between nodes  $v_i$  and  $v_j$ . Since a larger ( $Q$ ) leads to a better community partition, modularity maximization has become a popular approach in finding good community division [28].

Typically, modularity maximization can be viewed as a constrained optimization objective in the following form:

$$\begin{aligned} \max_{\mathbf{P}} \quad & Q := \text{tr}(\mathbf{P}^T \mathbf{B} \mathbf{P}), \\ \text{s.t.} \quad & \mathbf{P} \in \{0, 1\}^{N \times C}, \\ & \text{tr}(\mathbf{P}^T \mathbf{P}) = N, \end{aligned} \quad (2)$$

where  $\mathbf{B} \in \mathbb{R}^{N \times N}$  is the *modularity matrix*, with each element  $\mathbf{B}_{i,j} = \mathbf{A}_{i,j} - \frac{d_i d_j}{2m}$  the *modularity coefficient*.  $\mathbf{P} = \{p_1, p_2, \dots, p_N\} \in \{0, 1\}^{N \times C}$  is a one-hot matrix indicating the community ownership of each node in the graph, i.e., *community assignment matrix*. Typically,  $\mathbf{P}_{i,j} = 1$  if  $v_i$  belongs to community  $\mathcal{V}_j$  and 0 otherwise.

### 3.3 Connecting modularity maximization to contrastive learning

Based on the preliminary knowledge introduced above, we now provide our insights to demonstrate the underlying relationship between modularity maximization and contrastive learning. Formally, we rewrite Eq. (1) into an equivalent form below:

$$\begin{aligned} \max_{\mathbf{P}} \quad Q &:= \text{tr}(\mathbf{P}^T \mathbf{B} \mathbf{P}) = \frac{1}{2m} \sum_{i,j} \mathbf{B}_{i,j} p_i^T p_j \\ &= \frac{1}{2m} \left( \sum_{(v_i, v_j) \in \mathcal{M}^+} \mathbf{B}_{i,j} p_i^T p_j + \sum_{(v_i, v_j) \in \mathcal{M}^-} \mathbf{B}_{i,j} p_i^T p_j \right) \quad (3) \\ \text{s.t.} \quad p_i &\in \{0, 1\}^C \text{ and } p_i^T p_i = 1 \quad \forall i = 1, 2, \dots, N, \end{aligned}$$

where  $\mathcal{M}^+ = \{(v_i, v_j) | \mathbf{B}_{i,j} > 0\}$  and  $\mathcal{M}^- = \{(v_i, v_j) | \mathbf{B}_{i,j} \leq 0\}$  are positive and negative pairs, respectively. In this regard, modularity maximization is similar in form to graph autoencoders, with the goal of optimization is to reconstruct the modularity matrix  $\mathbf{B}$  rather than adjacency matrix  $\mathbf{A}$ . Motivated by a recent work [21] that showed the equivalence between graph autoencoders and contrastive learning, we provide our intuition to explicitly relate modularity maximization to contrastive learning.

Here we further unify Eq. (3) into a general form from the perspective of optimization. Since directly maximizing Eq. (3) is intractable, we can now relax  $\mathbf{P} \in \{0, 1\}^{N \times C}$  to its continuous analog  $\mathbf{Z} \in \mathbb{R}^{N \times C}$ , where  $\mathbf{Z}$  is node representations learned from a graph encoder  $f$  such that  $\mathbf{Z} = f(\mathcal{G})$ .

$$\begin{aligned} \max_{f, g} \quad Q &= \frac{1}{2m} \left( \sum_{(v_i, v_j) \in \mathcal{M}^+} \mathbf{B}_{i,j} z_i^T z_j + \sum_{(v_i, v_j) \in \mathcal{M}^-} \mathbf{B}_{i,j} z_i^T z_j \right) \\ &= \frac{1}{2m} \left( \sum_{(v_i, v_j) \in \mathcal{M}^+} |\mathbf{B}_{i,j}| z_i^T z_j - \sum_{(v_i, v_j) \in \mathcal{M}^-} |\mathbf{B}_{i,j}| z_i^T z_j \right) \quad (4) \\ &= \frac{1}{2m} \left( \sum_{(v_i, v_j) \in \mathcal{M}^+} g(z_i, z_j) - \sum_{(v_i, v_j) \in \mathcal{M}^-} g(z_i, z_j) \right), \end{aligned}$$

where  $g(\cdot, \cdot)$  is the decoder network that decodes the pairwise node representations  $(z_i, z_j)$  into the modularity score. Typically, the decoder  $g$  can be simply defined by cosine similarity function, i.e.,  $g(z_i, z_j) = z_i^T z_j$  or a neural network. Community coefficient  $\mathbf{B}_{i,j}$  is absorbed into  $g$  and  $f$  and should be adjusted by the neural network during training. According to Eq. (4), we obtain a general form of graph contrastive learning, where positive and negative pairs are guided by the modularity coefficient  $\mathbf{B}_{i,j}$ .

### 3.4 Opportunity: community-aware pretext task

As discussed in Section 1, current GCL methods for graph clustering, whether augmentation-based or augmentation-free, may face challenges related to scalability and/or semantic drift. Therefore, an alternative yet promising way is to utilize modularity maximization as a pretext task to generate community-aware pseudo-labels that guide contrastive learning. Specifically, the employment of the modularity matrix allows us to reveal the underlying community structure within the graph. In this regard, positive sample pairs are naturally defined as connected node pairs within the same community, while negative sample pairs are unconnected node pairs

from different communities. This leverages the intrinsic community structure in the network to mitigate the impact of semantic drift while also eliminating the need for graph augmentations that may hinder its scalability. Moreover, by establishing the relationship between modularity maximization and contrastive learning, we are able to integrate the latest advancements in modularity maximization into research on graph contrastive learning. Recent advances in the field of modularity maximization mainly include: (1) neural modularity maximization [2, 41]; (2) high-order proximity in modularity [23]; (3) Better parallel optimization algorithms [40], etc. The ones that are closely related to contrastive learning are (1) and (2). In this work, we propose to obtain cluster assignment via GNN encoder [14, 19], which allows (soft) cluster assignment to be differentiable for neural modularity maximization. In addition, we fully consider high-order proximity in modularity, and propose a sampling method based on random walk to ensure scalability while capturing high-order proximity within the community.

## 4 METHOD

In this section, we present an overview of the architecture of MAGI, which comprises a graph convolutional encoder, a two-stage random walk sampler that serves the modularity maximization pretext task, and a SimCLR [6] contrastive loss. Each of these components will be introduced separately in the following subsections.

### 4.1 GNN encoder

An encoder in GCL is a crucial component that maps the input graph data into latent representations. In MAGI, we employ different GNNs as encoders to encode graphs of varying sizes. Here we consider only two representative GNNs, i.e., GCN [19] and GraphSAGE [14]. It is important to note that MAGI is not specific to any particular GNN model and can be applied with other architectures (e.g., GAT [43]) as well.

**GCN.** GCN is a popular GNN model that has been widely used for various graph-based tasks. GCN operates by aggregating information from neighboring nodes and propagating it through multiple layers. It leverages the spectral graph convolution operation, which is based on the graph Laplacian matrix, to capture local and global graph structure. Formally, the message propagation of  $l$ -th layer in GCN is defined as:

$$h_u^{(l)} = \text{LeakyReLU} \left( \sum_{v \in \mathcal{N}_u \cup \{u\}} \frac{\mathbf{W}^{(l)} h_v^{(l-1)}}{\sqrt{(|\mathcal{N}_u| + 1)(|\mathcal{N}_v| + 1)}} \right), \quad (5)$$

where  $\text{LeakyReLU}(\cdot) = \max(0, \cdot) + \alpha * \min(0, \cdot)$  is activation function.  $\mathcal{N}_u$  is the set of adjacent neighbors of node  $u$ .  $\mathbf{W}$  is the learnable weight of layer  $l$  and  $h^{(l)}$  is the latent representation with  $h^{(0)} = x$ .

**GraphSAGE.** GCN relies on a symmetric and fixed aggregation function based on the graph Laplacian, which can limit its ability to capture diverse neighborhood structures and scale to large graphs effectively. GraphSAGE is a GNN alternative designed to better handle large-scale graphs in an inductive manner:

$$h_u^{(l)} = \text{LeakyReLU} \left( \mathbf{W}_1^{(l)} h_u^{(l-1)} + \mathbf{W}_2^{(l)} \Theta(\{h_v^{(l-1)} | v \in \mathcal{N}_u\}) \right), \quad (6)$$

where  $\Theta$  denotes different aggregation functions, such as mean, max, or LSTM-based aggregation. This allows GraphSAGE to capture diverse types of neighborhood information, accommodating various

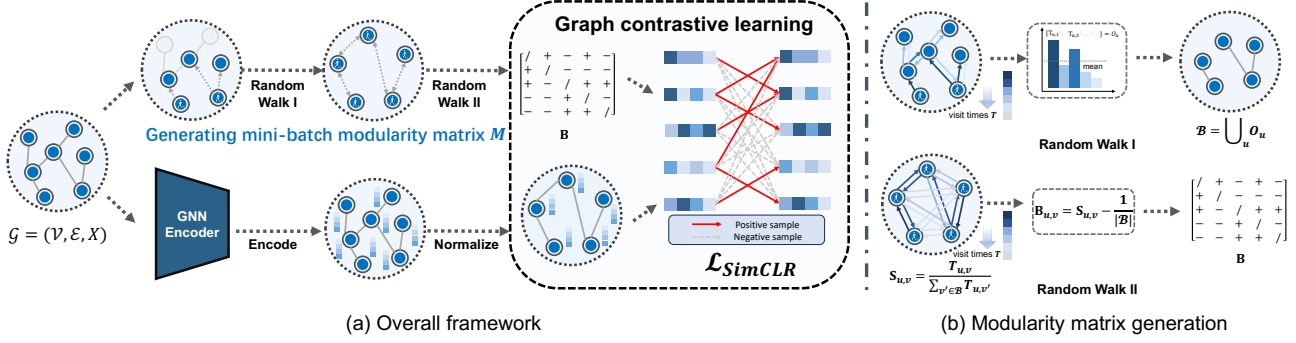


**Figure 2: Overview of proposed MAGI framework.** During the self-supervised learning phase, the original graph  $\mathcal{G}$  is provided to generate node embedding and modularity matrix through a GNN encoder and a two-stage random walk process, respectively. Then, the SimCLR loss function is employed to optimize the encoder in a self-supervised manner.

graph structures and improving its capability to learn from different node interactions.

## 4.2 Modularity maximization pretext task

The core insight behind neural modularity maximization is the computation of the modularity matrix  $\mathbf{B}$ . In order to adapt the minibatch training to obtain good scalability, an intuitive idea is to randomly sample  $n$  nodes in the graph and obtain contrastive pairs from their corresponding sub-modularity matrix. However, it is important to note that this approach potentially introduces the following issues:

- **Structure bias.** The sampled subgraph may not necessarily share a similar structure with the overall graph, which can hinder the performance of contrastive learning. Nevertheless, this issue becomes more serious as the graph becomes larger and sparser.
- **Lack of high-order proximity.** The vanilla modularity matrix only focuses on the first-order proximity within the graph, which contradicts our intuitive understanding of community structure in networks, that is, two nodes often belong to the same community due to high-order proximity, such as having many common neighbors. Although a recent work [23] explored the benefits brought by high-order proximity and used high-order polynomials of the adjacency matrix  $\mathbf{A}$  to calculate the high-order modularity matrix. However, the cost of computing high-order polynomials of the adjacency matrix  $\mathbf{A}$  for large-scale graphs is still prohibitive. We discuss the benefits of incorporating high-order proximity through experimental investigation in Section 6.2.

In this work, we propose a two-stage random walk-based sampling method to address the aforementioned challenges, as by adjusting the depth of the random walks, we can effectively capture the high-order proximity within the network. Specifically, we employ a first-stage random walk to sample multiple sub-communities and merge them into a training batch, ensuring that the corresponding subgraph within the batch contains effective community

structures to guide the model. Subsequently, we perform a second-stage random walk to generate a similarity matrix between nodes within the batch, and we draw on the concept of the configuration model [5] to calculate the corresponding modularity matrix in the mini-batch form.

Next, we will provide a detailed description of these two stages, which we refer to as **S1** and **S2**, respectively.

**(S1) Sampling multiple sub-communities.** For any  $v$  in set  $\mathcal{N}$  consisting of  $n$  randomly selected root nodes in the graph, based on the principle of internal connectivity within communities, there must be an overlap between the neighborhood of node  $v$  and its potential community, denoted as  $O_v$ . Accurately selecting  $O_v$  can be an expensive task because it involves detecting potential community structures in the graph. However, based on the definition that a *community is a set of nodes is densely connected internally*, we utilize random walks to approximate  $O_v$ . To be specific, we initiate  $t$  random walks of depth  $l$  rooted at node  $v$  and denote the set of visited nodes as  $\mathcal{U}_v^1$ , with the corresponding visit count recorded as  $T_v^1$ , which each element  $t_{v,u}^1$  as the number of visits from  $v$  to  $u$ . We filter  $O_v$  in the following way:

$$O_v = \{u \in \mathcal{U}_v^1 \mid t_{v,u}^1 > \frac{\sum_{u'} t_{v,u'}^1}{|\mathcal{U}_v^1|}\} \quad (7)$$

In brief, we consider nodes with visits greater than the mean as  $O_v$ . Then, for nodes in  $\mathcal{N}$ , we perform the same operation and set  $\mathcal{B} = \cup_{v \in \mathcal{N}} O_v$  as a training batch.

**(S2) Mini-batch modularity matrix.** It is intuitive to treat pair nodes from the same sub-community as positives and those from different sub-communities as negatives. However, we must consider the potential overlaps between different sub-community, necessitating further exploration of the relationships among nodes in  $\mathcal{B}$ . Specifically, we perform again  $t$  random walks of depth  $l$  for each node in  $\mathcal{B}$ . For any two nodes  $v$  and  $u$  in  $\mathcal{B}$ , let  $t_{v,u}^2$  be the number of visits from  $v$  to  $u$ , we can then construct a similarity matrix  $\mathbf{S}$  for the nodes in  $\mathcal{B}$  based on the number of visits, which each element:

$$S_{v,u} = \frac{t_{v,u}^2}{\sum_{u' \in \mathcal{B}} t_{v,u'}^2} \quad (8)$$

denotes probability that node  $v$  is connected to node  $u$ . Subsequently, following [27] we employ the configuration model [5] to estimate the expected probability of connection between any two nodes in  $\mathcal{B}$ . Ultimately, we get the mini-batch form of modularity matrix  $\mathbf{B}$ , where each element:

$$\mathbf{B}_{v,u} = S_{v,u} - \frac{\sum_{u' \in \mathcal{B}} S_{v,u'} \sum_{v' \in \mathcal{B}} S_{v',u}}{\sum_{v',u'} S_{v',u'}} = S_{v,u} - \frac{1}{|\mathcal{B}|} \quad (9)$$

### 4.3 Contrastive loss formulation

Given a train batch  $\mathcal{B}$  and corresponding modularity matrix  $\mathbf{B}$ , for any nodes  $v \in \mathcal{B}$ , set  $\mathcal{M}_v^+ = \{u \in \mathcal{B} | \mathbf{B}_{v,u} > 0\}$  and  $\mathcal{M}_v^- = \{u \in \mathcal{B} | \mathbf{B}_{v,u} \leq 0\}$  are the positive and negative samples of  $v$ , respectively. Now a simple contrastive loss used in Eq.(1) as:

$$\mathcal{L}_{simple}(v) = - \sum_{u \in \mathcal{M}_v^+} sim(z_v, z_u) + \sum_{u' \in \mathcal{M}_v^-} sim(z_v, z_{u'}), \quad (10)$$

where  $sim$  is inner product similarity function:  $sim(z_v, z_u) = \frac{z_v^T z_u}{\|z_v\| \|z_u\|}$ .

However, the above loss function demonstrates significantly inferior performance [45] compared to the softmax-based SimCLR contrastive loss [6], which formulated as:

$$\mathcal{L}_{SimCLR}(v) = - \sum_{u \in \mathcal{M}_v^+} \log \frac{\exp(z_v \cdot z_u / \tau)}{\sum_{u \in \mathcal{M}_v^+} \exp(z_v \cdot z_u / \tau) + \sum_{u' \in \mathcal{M}_v^-} \exp(z_v \cdot z_{u'} / \tau)} \quad (11)$$

The softmax-based SimCLR contrastive loss is a hardness-aware loss function [45], where  $\tau$  is temperature and plays a key role in controlling the local separation and global uniformity of the representation distributions. Appropriate temperature selection can effectively alleviate the uniform-tolerance dilemma. Based on the above analysis, we use the SimCLR loss function defined in Eq.(11) to learn the encoder.

### 4.4 Complexity analysis

The space complexity of our algorithm is  $O(Nd + m + b^2)$ , where  $N$  and  $m$  are the number of nodes and edges in the graph, respectively.  $d$  is the attribute dimension, and  $b$  is the batch size. For all datasets, we store the graph feature  $\mathbf{X}$ , the sparse adjacency matrix  $\mathbf{A}$ , and the mini-batch modularity matrix  $\mathbf{B}$  in memory, which require  $O(Nd)$ ,  $O(m)$ , and  $O(b^2)$  storage space, respectively. For GPUs, since only the subgraph data corresponding to each batch needs to be stored, the space complexity is reduced to  $O(b(b + d))$ . For a given batch, the forward and backward computation costs  $O(bd^2)$ . Hence, for  $N$  nodes, and  $r$  epochs, time complexity is  $O(Nrd^2)$ . We compare the time and space complexity of all methods used in Table 2, and the result (see Table 4 in Appendix) shows that MAGI performs better in terms of both time and memory complexity as compared to other methods that leverage both graph and feature information.

## 5 EXPERIMENTS

In this section, we conducted extensive experiments on several node classification benchmark datasets to evaluate the performance of our method in comparison with state-of-the-art baselines. Code is made publicly available at <https://github.com/EdisonLeeeee/MAGI>.

### 5.1 Datasets

In our experiments, we employ four small scale datasets (Cora [19], Citeseer [19], Photo [34], Computers [34]), three large scale datasets

**Table 1: Dataset statistics.**

Dataset	# Nodes	# Edges	# Features	# Clusters
Cora	2,708	5,278	1,433	7
CiteSeer	3,327	4,614	3,703	6
Amazon-Photo	7,650	119,081	745	8
Amazon-Computers	13,752	491,722	767	10
ogbn-arxiv	169,343	1,166,243	128	40
Reddit	232,965	23,213,838	602	41
ogbn-products	2,449,029	61,859,140	100	47
ogbn-papers100M	111,059,956	1,615,685,872	128	172

(Reddit [14], ogbn-arxiv [17], ogbn-products [17]) and one extra-large scale dataset (ogbn-papers100M [17]) to showcase the effectiveness of our method. The details of the datasets are presented in Table 1.

### 5.2 Baselines

We compare MAGI with 11 baselines, which can be categorized into five groups:

- (1) **Methods utilize graph structure only.** Node2vec [12] is a scalable graph embedding technique that utilizes random walks on the graph structure.
- (2) **Methods utilize graph features only.** K-means[25] is a traditional clustering algorithms that utilize only graph features.
- (3) **GCLs with augmentations.** DGI [44], GRACE [51], MV-GRL [15] and BGRL [39] are GCLs based on data augmentation to learn node representations.
- (4) **Augmentation-free GCLs.** CCGC [48], SCGDN [24], and S<sup>3</sup>GC [9] are recent augmentation-free GCLs.
- (5) **Methods based on neural modularity maximization.** DGCLUSTER [2] and DMoN [41] are two recent neural modularity maximization methods that can achieve good performance in graph clustering, in which DGCLUSTER is a semi-supervised method.

### 5.3 Metrics

Following the evaluation setup of [9, 15], we measure 4 metrics related to evaluating the quality of cluster assignments: Accuracy (ACC), Normalized Mutual Information (NMI), Adjusted Rand Index (ARI) and Macro-F1 Score (F1). For all the aforementioned metrics, higher values indicate better clustering performance. In our experiments, we first generate representations for each method and then perform spectral clustering on the embeddings of small-scale datasets (Cora, Citeseer, Photo, Computers) and K-means clustering on the other datasets to produce cluster assignments for evaluation.

### 5.4 Experimental setup

We use a single NVIDIA A100 GPU with 40GB memory for each method. All experiments are repeated 5 times and the mean values are reported in Table 2. For all datasets except for ogbn-papers100M, we set the number of run epochs at 400 and limit the maximum runtime to 1 hour. For ogbn-papers100M we allow up to 6 hours of training in addition to 256GB memory limitation. We employ full batch training on small-scale graphs and set the number of rooted nodes  $n$  as 2048 for large and extra-large datasets. Due to space limitations, more details about the hyperparameters are mentioned

**Table 2: Clustering performance of MAGI and 11 state-of-the-art baselines. The boldfaced score and underlined score indicate the best and second-best results, respectively. “OOM” denotes out-of-memory, and \* indicates semi-supervised method.**

Method	Metric	Baselines											Ours
		K-means	Node2vec	DGI	GRACE	MVGRL	BGRL	CCGC	SCGDN	DGCLUSTER*	S <sup>3</sup> GC	DMoN	MAGI
Cora	ACC	0.350	0.612	0.726	0.739	<b>0.763</b>	0.742	0.664	0.748	0.753	0.742	0.517	<u>0.760</u>
	NMI	0.173	0.444	0.571	0.570	<b>0.608</b>	0.584	0.527	0.569	0.600	0.588	0.473	<u>0.597</u>
	ARI	0.127	0.329	0.511	0.527	<u>0.566</u>	0.534	0.446	0.526	0.548	0.544	0.301	<b>0.573</b>
	F1	0.360	0.621	0.692	<u>0.725</u>	0.716	0.691	0.587	0.704	0.706	0.721	0.574	<b>0.739</b>
Citeseer	ACC	0.421	0.421	0.686	0.631	<u>0.703</u>	0.675	0.664	0.696	0.618	0.688	0.385	<b>0.706</b>
	NMI	0.199	0.240	0.435	0.399	<b>0.459</b>	0.422	0.418	0.443	0.373	0.441	0.303	<u>0.452</u>
	ARI	0.142	0.116	0.445	0.377	<b>0.471</b>	0.428	0.414	0.454	0.322	0.448	0.200	<u>0.468</u>
	F1	0.394	0.401	0.643	0.603	<b>0.654</b>	0.631	0.627	0.655	0.543	0.643	0.437	<u>0.648</u>
Photo	ACC	0.272	0.276	0.430	0.677	0.411	0.665	0.689	0.780	<b>0.820</b>	0.752	0.248	<u>0.790</u>
	NMI	0.132	0.115	0.337	0.535	0.303	0.601	0.612	0.694	<b>0.735</b>	0.598	0.077	<u>0.716</u>
	ARI	0.055	0.049	0.221	0.427	0.188	0.441	0.495	0.607	<b>0.671</b>	0.561	0.038	<u>0.615</u>
	F1	0.240	0.215	0.352	0.503	0.329	0.631	0.609	0.716	<b>0.752</b>	0.729	0.180	<u>0.729</u>
Computers	ACC	0.225	0.356	0.479	0.519	0.580	0.469	0.480	0.582	0.453	<u>0.588</u>	0.432	<b>0.620</b>
	NMI	0.110	0.278	0.420	0.538	0.482	0.441	0.452	0.545	0.498	<u>0.560</u>	0.461	<b>0.592</b>
	ARI	0.056	0.248	0.306	0.343	0.433	0.306	0.290	0.430	0.261	<u>0.438</u>	0.288	<b>0.462</b>
	F1	0.152	0.224	0.390	0.390	0.405	0.415	0.380	0.480	0.372	<u>0.475</u>	0.390	<b>0.574</b>
ogbn-arxiv	ACC	0.181	0.290	0.314							<u>0.350</u>	0.250	<b>0.388</b>
	NMI	0.221	0.406	0.412	OOM	OOM	OOM	OOM	OOM	OOM	<u>0.463</u>	0.356	<b>0.469</b>
	ARI	0.074	0.190	0.223	OOM	OOM	OOM	OOM	OOM	OOM	<u>0.270</u>	0.127	<b>0.310</b>
	F1	0.129	0.220	<u>0.230</u>							<u>0.230</u>	0.190	<b>0.266</b>
Reddit	ACC	0.089	0.709	0.224							<u>0.736</u>	0.529	<b>0.911</b>
	NMI	0.114	0.792	0.306	OOM	OOM	OOM	OOM	OOM	OOM	<u>0.807</u>	0.628	<b>0.875</b>
	ARI	0.029	0.640	0.170	OOM	OOM	OOM	OOM	OOM	OOM	<u>0.745</u>	0.502	<b>0.907</b>
	F1	0.068	0.551	0.183							<u>0.560</u>	0.260	<b>0.853</b>
ogbn-products	ACC	0.200	0.357	0.320							<u>0.402</u>	0.304	<b>0.425</b>
	NMI	0.273	0.489	0.467	OOM	OOM	OOM	OOM	OOM	OOM	<u>0.536</u>	0.428	<b>0.551</b>
	ARI	0.082	0.170	0.174	OOM	OOM	OOM	OOM	OOM	OOM	<b>0.230</b>	0.139	<u>0.215</u>
	F1	0.124	0.247	0.192							<u>0.250</u>	0.210	<b>0.276</b>

in Table 5 in the Appendix. We have provided a mini-batch and highly scalable implementation of MAGI in PyTorch, making it easy for experiments with all datasets to adapt to GPU processing. For all datasets, it is only need to store the subgraphs and corresponding modularity matrix in a sparse form to execute MAGI’s *forward* and *backward* pass on the GPU. We also provide the GPU memory cost and the time required to execute the training process for each method in Table 4 in Appendix.

## 6 EXPERIMENTAL RESULTS

In this section, we present the experimental results of MAGI in the graph clustering task. In addition to the main experiments, we have conducted supplementary experiments aimed at answering the following research questions:

(Q1): Can MAGI scale to extra-large scale graphs containing up to 100 million nodes and outperform state-of-the-art baselines?

(Q2): Can modularity maximization pretext tasks effectively mitigate the problem of semantic drift?

(Q3): Is MAGI robust to different hyperparameters, and does each mechanism within MAGI contribute uniquely to its performance?

**Table 3: Comparison results of different scalable methods on ogbn-papers100M with 111M nodes and 1.6B edges.**

	ogbn-papers100M			
	Accuracy	NMI	ARI	F1
<b>K-means</b>	0.144	0.368	0.074	<u>0.101</u>
<b>Node2vec</b>	<u>0.175</u>	0.380	<u>0.112</u>	0.099
<b>DGI</b>	0.151	0.416	0.096	0.111
<b>S<sup>3</sup>GC</b>	0.173	<u>0.453</u>	0.110	<b>0.118</b>
<b>MAGI</b>	<b>0.288</b>	<b>0.463</b>	<b>0.207</b>	0.096

### 6.1 Graph clustering result

Table 2 presents a comparison of MAGI’s clustering performance against various baseline methods across different scale datasets. For

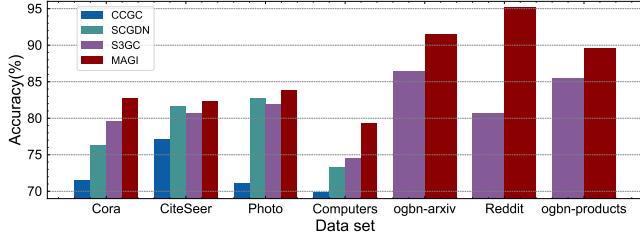


Figure 3: Comparison of pseudo-labels constructed by MAGI and other methods.

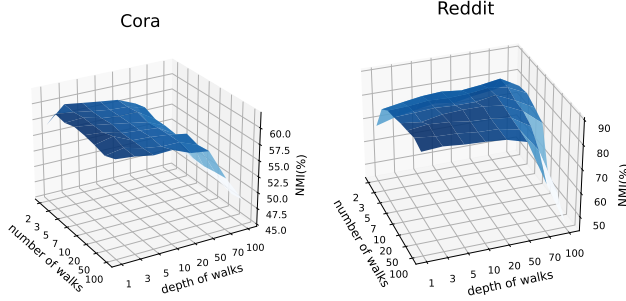


Figure 4: The performance of MAGI with varying the number and depth of random walks on the Cora and Reddit dataset in terms of NMI.

small-scale datasets, namely Cora, Citeseer, Photo, and Computers, we observe that MVGRL,  $S^3GC$ , and DGCLUSTER emerge as the three strongest baseline methods. Nonetheless, we find that MAGI consistently ranks first or second in performance in most cases. We note that even when compared to semi-supervised methods such as DGCLUSTER, MAGI is only slightly behind on the Photo dataset and maintains a consistent lead on the other three datasets, demonstrating MAGI’s superior performance. Next, we observe the performance on large-scale datasets and find that MAGI notably outperforms baseline methods like DGI, DMoN and  $S^3GC$ . MAGI is  $\sim 3.6\%$  better on ogbn-arxiv,  $\sim 29\%$  better on Reddit and  $\sim 2.6\%$  better on ogbn-products in terms of clustering F1 as compared to the second-best method. Significantly, MAGI outperforms the second-best method on the Reddit dataset with an approximate increase of  $\sim 18\%$  in Accuracy,  $\sim 7\%$  in NMI,  $\sim 16\%$  in ARI, and  $\sim 29\%$  in F1 score. One possible reason for the superior performance is that the Reddit dataset exhibits a higher graph density, which results in a more distinct community structure.

**ogbn-papers100M:** To answer Q1, we conduct a comparative analysis of MAGI’s performance on an extra-large dataset containing 111M nodes and 1.6B edges. Note that we compare K-means, Node2vec, DGI, and  $S^3GC$  since others can not scale to this dataset. The results are presented in Table 3. Our experimental results reveal that MAGI adeptly scales to this dataset and demonstrates a significant performance improvement over methods relying solely on features (K-means) by approximately  $\sim 14.4\%$ , exclusively on

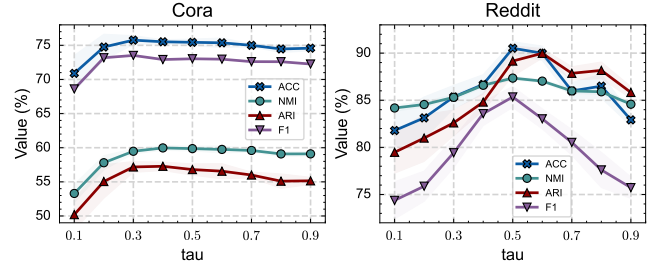


Figure 5: The performance of MAGI with varying the temperature  $\tau$  on the Cora and Reddit dataset, respectively.

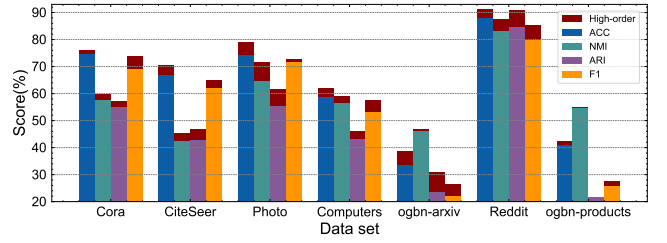


Figure 6: Benefits of incorporating high-order proximity, with the red part of each bar representing the gains provided by high-order proximity.

graph structure (Node2vec) by approximately  $\sim 11.3\%$ , and both features and structure ( $S^3GC$ ) by approximately  $\sim 11.5\%$  in terms of accuracy on the ogbn-papers100M dataset.

## 6.2 Semantic drift mitigation

In practice, it is difficult to measure the degree of semantic drift in a graph. To answer Q2, we alternatively measure the semantic drift based on the quality of pseudo-labels generated by various methods. Specifically, considering the augmentation-free GCLs referenced in Section 5.2, we employ ground-truth labels to evaluate the accuracy of pseudo-labels produced by these methods. In this context, a positive sample pair is considered as ‘1’ if both nodes belong to the same class, while a negative sample pair is deemed ‘1’ if the nodes belong to different classes; otherwise, they are labeled as ‘0’. The results (refer to Figure 3) demonstrate that, in comparison to other augmentation-free GCLs, MAGI generates higher-quality pseudo-labels. This confirms the efficacy of modularity maximization as a pretext task in mitigating semantic drift.

## 6.3 Ablation study

To answer Q3, we first conduct thorough ablation studies on hyperparameters including the number of walks  $t$ , depth of walks  $l$ , number of randomly rooted nodes  $n$  and temperature  $\tau$  to examine the stability of MAGI’s clustering. Our findings are listed below:

(1) The performance of MAGI remains relatively stable as long as the number and depth of random walks are not excessively extreme, as shown in Figure 4. We also note that the walk depth  $\sim 5$  is an optimal choice, as a larger walk depth tends to sample positive pairs



Figure 7: *t*-SNE visualization of eight unsupervised methods on the Photo dataset.

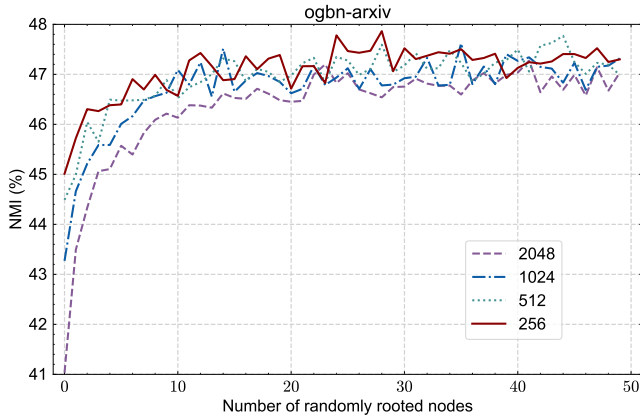


Figure 8: The performance of MAGI with varying different number of randomly rooted nodes  $n$  on the ogbn-arxiv dataset in terms of NMI.

with differing community semantics. This finding is consistent with the previous work [9].

(2) MAGI can achieve the best performance when the temperature  $\tau$  is around  $\sim 0.5$  (see Figure 5). A temperature  $\tau$  that is too small or too large can lead to the model paying too much or too little attention to hard negative samples [45], respectively.

(3) Different number of randomly sampled root nodes  $n$  have similar clustering performance, but a smaller  $n$  can lead to faster convergence (see Figure 8). Combined with MAGI’s stable performance at smaller walk depths, this demonstrates MAGI’s good scalability, meaning that for each node, MAGI only needs to sample a few positive samples.

**High-order proximity.** We then showcase the effectiveness of exploring high-order proximity in MAGI. In a given batch  $\mathcal{B}$ , the effectiveness of employing random walks versus directly sampling a submatrix from the vanilla modularity matrix is compared across various datasets. Figure 6 demonstrates that, in the majority of cases, the use of random walks outperforms direct sampling. This result highlights the advantage of incorporating high-order proximity into the analysis, enabling a better capture of the complex relationships and community structure within the graph.

**Effectiveness of different components.** We conduct ablation study to manifest the efficacy of different components in MAGI. We set five variants of our model for comparison. Results are shown in Table 6 in Appendix, where “MAGI (w/ SL)” refers to the use of simple contrastive loss defined in Eq.( 10), “MAGI (w/ MS)” refers to use  $\mathbf{S1}$  and the sign of modularity score to define positive and negative sample sets, “MAGI (w/ EI)” refers to use  $\mathbf{S1}$  and edge indicators to define positive and negative sample sets, “MAGI (w/

HMS)” refers to use sign of high-order modularity score [23] to define positive and negative sample sets and MAGI refers to use  $\mathbf{S1}$  and  $\mathbf{S2}$  to define positive and negative sample sets.

In Table 6, it is observed that each improvement of our model contributes to the final performance. First, loss (11) performs better than loss (10). Secondly, the direct use of edge indicators to define the positive and negative sample sets achieves the worst effect. We infer that this may be because some edges exist between different communities, which leads to some positive sample pairs from different communities, increasing the impact of semantic drift. This can be mitigated by the use of modularity scores, and consideration of high-order proximity in the community can further eliminate the impact of semantic drift. Finally, our sampling strategy achieves similar performance compared to using the sign of high order modularity matrix proposed in [23], but our sampling strategy has lower computational complexity and can be scaled to large-scale graph datasets with 100M nodes.

## 6.4 Visualization

In this part, we measure the quality of the generated embeddings by directly employing *t*-SNE [42]. The generated embeddings of each method are projected into 2-dimensional vectors for visualization. Due to space limitations, we have selected seven strong baseline methods for visual analysis. It should also be noted that DGCLUSTER [2], being a semi-supervised method, was excluded from this comparison. The visualization clearly demonstrates that MAGI produces representations with significantly higher clustering efficacy compared to baseline methods.

## 7 CONCLUSION

In this paper, we explore the problem of graph clustering via neural modularity maximization. Our work establishes the connection between neural modularity maximization and graph contrastive learning. This insight motivates us to propose MAGI, a community-aware graph clustering framework with modularity maximization as the pretext task for contrastive learning. MAGI is an augmentation-free GCL framework, which avoids potential semantic drift and scalability issues. To ensure better scalability, MAGI adopts a two-stage random walk to approximate the modularity matrix in a mini-batch manner, followed by a principled contrastive loss to optimize the goal of modularity maximization. Extensive experiments on eight real-world graph datasets demonstrate the effectiveness of our method, which achieves state-of-the-art in most cases compared with strong baselines. We hope that the straightforward nature of our approach serves as a reminder to the community to reevaluate simpler alternatives that may have been overlooked, thereby inspiring future research.

## REFERENCES

- [1] Vandana Bhatia and Rinkle Rani. 2018. DFuzzy: a deep learning-based fuzzy clustering model for large graphs. *Knowledge and Information Systems* 57 (2018), 159–181.
- [2] Aritra Bhowmick, Mert Kosan, Zexi Huang, Ambuj K. Singh, and Sourav Medya. 2024. DGCLUSTER: A Neural Framework for Attributed Graph Clustering via Modularity Maximization. In *AAAI AAAI Press*, 11069–11077.
- [3] Vincent D Blondel, Jean-Loup Guillaume, Renaud Lambiotte, and Etienne Lefevre. 2008. Fast unfolding of communities in large networks. *Journal of statistical mechanics: theory and experiment* 2008, 10 (2008), P10008.
- [4] Ulrik Brandes, Daniel Delling, Marco Gaertler, Rachelle Goerke, Martin Hoefler, Zoran Nikoloski, and Donald Wagner. 2006. Maximizing Modularity is hard. *arXiv: Data Analysis, Statistics and Probability* (2006).
- [5] Markus Brede. 2012. *Networks—An Introduction*. Mark E. J. Newman. (2010, Oxford University Press.) \$65.38, £35.96 (hardcover), 772 pages. ISBN-978-0-19-920665-0. *Artificial Life* 18 (2012), 241–242.
- [6] Ting Chen, Simon Kornblith, Mohammad Norouzi, and Geoffrey Hinton. 2020. A simple framework for contrastive learning of visual representations. In *ICML*. Article 149, 11 pages.
- [7] Jun Jin Choong, Xin Liu, and Tsuyoshi Murata. 2018. Learning Community Structure with Variational Autoencoder. In *ICDM*. 69–78.
- [8] Ganqu Cui, Jie Zhou, Cheng Yang, and Zhiyuan Liu. 2020. Adaptive Graph Encoder for Attributed Graph Embedding. In *KDD*. 976–985.
- [9] Fnu Devvrit, Aditya Sinha, Inderjit S Dhillon, and Prateek Jain. 2022. S3GC: Scalable Self-Supervised Graph Clustering. In *NeurIPS*, Alice H. Oh, Alekh Agarwal, Danielle Belgrave, and Kyunghyun Cho (Eds.).
- [10] Pedro F. Felzenszwalb and Daniel P. Huttenlocher. 2004. Efficient Graph-Based Image Segmentation. *International Journal of Computer Vision* 59 (2004), 167–181.
- [11] Jean-Bastien Grill, Florian Strub, Florent Altché, Corentin Tallec, Pierre H. Richemond, Elena Buchatskaya, Carl Doersch, Bernardo Avila Pires, Zhaohan Daniel Guo, Mohammad Gheslghi Azar, Bilal Piot, Koray Kavukcuoglu, Rémi Munos, and Michal Valko. 2020. Bootstrap your own latent a new approach to self-supervised learning. In *NeurIPS*. 14 pages.
- [12] Aditya Grover and Jure Leskovec. 2016. node2vec: Scalable Feature Learning for Networks. In *KDD*. Association for Computing Machinery, 855–864.
- [13] R. Hadsell, S. Chopra, and Y. LeCun. 2006. Dimensionality Reduction by Learning an Invariant Mapping. In *2006 IEEE Computer Society Conference on Computer Vision and Pattern Recognition (CVPR'06)*, Vol. 2. 1735–1742.
- [14] William L. Hamilton, Rex Ying, and Jure Leskovec. 2017. Inductive Representation Learning on Large Graphs. In *NeurIPS*. 1025–1035.
- [15] Kaveh Hassani and Amir Hosein Khasahmadi. 2020. Contrastive multi-view representation learning on graphs. In *ICML (ICML'20)*. JMLR.org, Article 385, 11 pages.
- [16] R Devon Hjelm, Alex Fedorov, Samuel Lavoie-Marchildon, Karan Grewal, Phil Bachman, Adam Trischler, and Yoshua Bengio. 2019. Learning deep representations by mutual information estimation and maximization. In *ICLR*.
- [17] Weihua Hu, Matthias Fey, Marinka Zitnik, Yuxiao Dong, Hongyu Ren, Bowen Liu, Michele Catasta, and Jure Leskovec. 2020. Open Graph Benchmark: Datasets for Machine Learning on Graphs. In *NeurIPS*.
- [18] Thomas N Kipf and Max Welling. 2016. Variational Graph Auto-Encoders. *NeurIPS Workshop on Bayesian Deep Learning* (2016).
- [19] Thomas N. Kipf and Max Welling. 2017. Semi-Supervised Classification with Graph Convolutional Networks. In *ICLR*.
- [20] Namkyeong Lee, Junseok Lee, and Chanyoung Park. 2022. Augmentation-Free Self-Supervised Learning on Graphs. (2022).
- [21] Jintang Li, Ruofan Wu, Wangbin Sun, Liang Chen, Sheng Tian, Liang Zhu, Changhua Meng, Zibin Zheng, and Weiqiang Wang. 2023. What's Behind the Mask: Understanding Masked Graph Modeling for Graph Autoencoders. In *KDD*. ACM, 1268–1279.
- [22] Jintang Li, Huizhe Zhang, Ruofan Wu, Zulun Zhu, Baokun Wang, Changhua Meng, Zibin Zheng, and Liang Chen. 2024. A Graph is Worth 1-bit Spikes: When Graph Contrastive Learning Meets Spiking Neural Networks. In *ICLR*.
- [23] Yunfei Liu, Zhen Liu, Xiaodong Feng, and Zhongyi Li. 2022. Robust Attributed Network Embedding Preserving Community Information. In *ICDE*. 1874–1886.
- [24] Yixuan Ma and Kun Zhan. 2023. Self-Contrastive Graph Diffusion Network. In *ACM MM*. 3857–3865.
- [25] J. MacQueen. 1967. Some methods for classification and analysis of multivariate observations.
- [26] Parham Moradi, Sajad Ahmadian, and Fardin Akhlaghian. 2015. An effective trust-based recommendation method using a novel graph clustering algorithm. *Physica A Statistical Mechanics and its Applications* 436 (2015), 462–481.
- [27] Mark EJ Newman. 2006. Modularity and community structure in networks. *Proceedings of the national academy of sciences* 103, 23 (2006), 8577–8582.
- [28] M. E. J. Newman. 2006. Finding community structure in networks using the eigenvectors of matrices. *Phys. Rev. E* (Sep 2006), 036104.
- [29] Shirui Pan, Ruiqi Hu, Sai-Fu Fung, Guodong Long, Jing Jiang, and Chengqi Zhang. 2020. Learning Graph Embedding With Adversarial Training Methods. *IEEE Transactions on Cybernetics* 50, 6 (2020), 2475–2487.
- [30] Jiwoong Park, Minsik Lee, Hyung Jin Chang, Kyuewang Lee, and Jin Young Choi. 2019. Symmetric Graph Convolutional Autoencoder for Unsupervised Graph Representation Learning. In *ICCV*. 6518–6527.
- [31] Advait Parulekar, Liam Collins, Karthikeyan Shanmugam, Aryan Mokhtari, and Sanjay Shakkottai. 2023. InfoNCE Loss Provably Learns Cluster-Preserving Representations. In *Annual Conference Computational Learning Theory*.
- [32] Bryan Perozzi, Rami Al-Rfou, and Steven Skiena. 2014. DeepWalk: Online Learning of Social Representations. In *KDD*. 701–710.
- [33] Guillaume Salha-Galvan, Johannes F. Lutzeyer, George Dasoulas, Romain Hennequin, and Michalis Vazirgiannis. 2022. Modularity-aware graph autoencoders for joint community detection and link prediction. *Neural Networks* 153 (2022), 474–495.
- [34] Oleksandr Shchur, Maximilian Mumme, Aleksandar Bojchevski, and Stephan Günnemann. 2018. Pitfalls of Graph Neural Network Evaluation. *ArXiv abs/1811.05868* (2018).
- [35] Jianbo Shi and J. Malik. 2000. Normalized cuts and image segmentation. *IEEE Transactions on Pattern Analysis and Machine Intelligence* 22, 8 (2000), 888–905.
- [36] Heli Sun, Fang He, Jianbin Huang, Yizhou Sun, Yang Li, Chenyu Wang, Liang He, Zhongbin Sun, and Xiaolin Jia. 2020. Network Embedding for Community Detection in Attributed Networks. *ACM Trans. Knowl. Discov. Data* 14, 3, Article 36 (may 2020), 25 pages.
- [37] Jianyong Sun, Wei Zheng, Qingfu Zhang, and Zongben Xu. 2022. Graph Neural Network Encoding for Community Detection in Attribute Networks. *IEEE Transactions on Cybernetics* 52, 8 (2022), 7791–7804.
- [38] Wangbin Sun, Jintang Li, Liang Chen, Bingzhe Wu, Yatao Bian, and Zibin Zheng. 2024. Rethinking and Simplifying Bootstrapped Graph Latents. In *WSDM*. ACM, 665–673.
- [39] Shantanu Thakoor, Corentin Tallec, Mohammad Gheslghi Azar, Rémi Munos, Petar Veličković, and Michal Valko. 2021. Bootstrapped Representation Learning on Graphs. In *ICLR 2021 Workshop on Geometrical and Topological Representation Learning*.
- [40] V. Traag, L. Waltman, and Nees Jan van Eck. 2019. From Louvain to Leiden: guaranteeing well-connected communities. *Scientific Reports* 9 (03 2019), 5233.
- [41] Anton Tsitsulin, John Palowitch, Bryan Perozzi, and Emmanuel Müller. 2023. Graph Clustering with Graph Neural Networks. *J. Mach. Learn. Res.* 24 (2023), 127:1–127:21.
- [42] Laurens van der Maaten and Geoffrey Hinton. 2008. Visualizing Data using t-SNE. *JMLR* 9, 86 (2008), 2579–2605.
- [43] Petar Veličković, Guillem Cucurull, Arantxa Casanova, Adriana Romero, Pietro Liò, and Yoshua Bengio. 2018. Graph Attention Networks. In *ICLR*.
- [44] Petar Veličković, William Fedus, William L. Hamilton, Pietro Liò, Yoshua Bengio, and R Devon Hjelm. 2019. Deep Graph Infomax. In *ICLR*.
- [45] Feng Wang and Huaping Liu. 2021. Understanding the Behaviour of Contrastive Loss. In *CVPR*. 2495–2504.
- [46] Zhirong Wu, Yuanjun Xiong, Stella X. Yu, and Dahua Lin. 2018. Unsupervised Feature Learning via Non-parametric Instance Discrimination. In *2018 IEEE/CVF Conference on Computer Vision and Pattern Recognition*. 3733–3742.
- [47] Liang Yang, Xiaochun Cao, Dongxiao He, Chuan Wang, Xiao Wang, and Weixiong Zhang. 2016. Modularity based community detection with deep learning. In *IJCAI (IJCAI'16)*. 2252–2258.
- [48] Xihong Yang, Yue Liu, Sihang Zhou, Siwei Wang, Wenxuan Tu, Qun Zheng, Xinwang Liu, Liming Fang, and En Zhu. 2023. Cluster-Guided Contrastive Graph Clustering Network. In *AAAI AAAI Press*, 9 pages.
- [49] Yuning You, Tianlong Chen, Yongduo Sui, Ting Chen, Zhangyang Wang, and Yang Shen. 2020. Graph Contrastive Learning with Augmentations. In *NeurIPS*, Vol. 33. 5812–5823.
- [50] Cangqi Zhou, Yuxiang Wang, Jing Zhang, Jiqiong Jiang, and Dianming Hu. 2022. End-to-end Modularity-based Community Co-partition in Bipartite Networks. In *CIKM*. 2711–2720.
- [51] Yanqiao Zhu, Yichen Xu, Feng Yu, Qiang Liu, Shu Wu, and Liang Wang. 2020. Deep Graph Contrastive Representation Learning. In *ICML Workshop on Graph Representation Learning and Beyond*.

## A ALGORITHM

To help better understand the proposed framework, we provide the detailed algorithm for training MAGI in Algorithm 1.

---

### Algorithm 1 Community-Aware Graph Clustering (MAGI)

---

**Input:** Graph  $\mathcal{G} = (\mathcal{V}, \mathcal{E}, \mathbf{X})$ , encoder  $f_\theta(\cdot)$ , Randomly sampled node set  $\mathcal{N}$ , number of walks  $t$ , depth of walks  $l$ , hyperparameter  $\alpha$ ;

**Output:** Learned encoder  $f_\theta(\cdot)$ ;

- 1: **while not converged do**
  - 2:   Perform random walk for each node in  $\mathcal{N}$ , obtain  $\mathcal{B}$ ;
  - 3:   Perform random walk for each node in  $\mathcal{B}$ , obtain similarity matrix  $\mathbf{S}$ ;
  - 4:   Calculate modularity matrix  $\mathbf{B}$  according to Eq.(9);
  - 5:   Calculate  $\mathcal{L}_{SimCLR}$  according to Eq.(11);
  - 6:   Update  $\theta$  by gradient descent;
  - 7: **end while**
  - 8: **return**  $f_\theta(\cdot)$ ;
- 

## B MORE DETAILS ABOUT THE COMPLEXITY ANALYSIS

We report the complexity analysis from both theoretical and experimental perspectives in Table 4.

## C MORE DETAILS ABOUT THE EXPERIMENTS

### C.1 Hyperparameter settings

We report our hyperparameter settings in Table 5.

### C.2 Ablation study on different mechanisms

We report the ablation study results on different mechanisms in Table 6.

**Table 4: Time and space analyses of different methods. Where  $k$  is the number of clusters. The experimental GPU memory costs and time costs (training) are obtained on Cora dataset.**

Method	Time Complexity	Space Complexity	Memory Cost(MB)	Time Cost(s)
Node2vec	$O(bd)$	$O(Nd)$	1,122	62.1
DGI	$O(md + Nd^2)$	$O(m + Nd + d^2)$	218	36.8
GRACE	$O(N^2d + md + d^2)$	$O(m + Nd)$	277	2.9
BGRL	$O(md + Nd^2)$	$O(m + Nd + d^2)$	1,201	31.2
MVGRL	$O(N^2d + Nd^2)$	$O(N^2 + Nd + d^2)$	2,924	33.9
SCGDN	$O(N^2 + Nd^2)$	$O(N^2 + Nd + d^2)$	1,080	31.9
CCGC	$O(kNd + N^2d + Nd^2)$	$O(N^2 + (N+k)d + d^2)$	3,233	38.0
DGCLUSTER	$O(N^2d + Nd^2)$	$O(N^2 + Nd + d^2)$	267	6.5
DMoN	$O((m+N)k)$	$O(m + Nk)$	301	9.3
S <sup>3</sup> GC	$O(Nsd^2)$	$O(Nd + bsd + d^2)$	2,148	27.2
MAGI	$O(Nd^2)$	$O(m + Nd + b^2)$	209	2.7

**Table 5: Hyperparameter settings, where  $d$  is the embedding dimension,  $\alpha$  is the activation threshold,  $\tau$  is the temperature,  $t$  is the number of random walks,  $l$  is the depth of random walks.**

Dataset	#GNN layers	$d$	$\alpha$	$\tau$	$t$	$l$	learning rate	weight decay
Cora	1	512	0.5	0.3	100	2	0.0005	0.001
CiteSeer	2	512	0.5	0.9	100	3	0.0001	0.0005
Photo	1	512	0.5	0.5	100	3	0.0005	0.001
Computers	2	512	0.1	0.9	100	3	0.0005	0.001
ogbn-arxiv	2	256	0.1	0.9	20	5	0.01	0
Reddit	2	256	0.5	0.5	20	5	0.01	0
ogbn-products	3	256	0.1	0.9	20	4	0.01	0
ogbn-papers100M	2	64	0.1	0.9	20	3	0.01	0

**Table 6: Ablations on different components of MAGI.**

Dataset	Metric	MAGI (w/ SL)	MAGI (w/ MS)	MAGI (w/ EI)	MAGI (w/ HMS)	MAGI
Cora	ACC	0.703	<u>0.754</u>	0.723	0.753	<b>0.760</b>
	NMI	0.541	0.582	0.562	<u>0.589</u>	<b>0.597</b>
	ARI	0.492	0.559	0.518	<u>0.561</u>	<b>0.573</b>
	F1	0.687	<u>0.736</u>	0.713	0.729	<b>0.739</b>
CiteSeer	ACC	0.701	0.700	<u>0.703</u>	0.698	<b>0.706</b>
	NMI	<b>0.452</b>	0.446	0.447	<u>0.448</u>	<b>0.452</b>
	ARI	<u>0.462</u>	0.459	0.443	0.443	<b>0.468</b>
	F1	0.645	<b>0.653</b>	0.632	0.639	<u>0.648</u>
Photo	ACC	0.672	0.749	0.736	<u>0.769</u>	<b>0.790</b>
	NMI	0.594	0.645	0.634	<u>0.683</u>	<b>0.716</b>
	ARI	0.473	0.562	0.541	<u>0.576</u>	<b>0.615</b>
	F1	0.684	<u>0.715</u>	0.713	0.706	<b>0.729</b>
Computers	ACC	0.496	0.590	0.590	<b>0.639</b>	<u>0.620</u>
	NMI	0.548	0.580	0.574	<b>0.604</b>	<u>0.592</u>
	ARI	0.342	0.438	0.432	<b>0.475</b>	<u>0.462</u>
	F1	0.395	0.558	0.543	<b>0.580</b>	<u>0.574</u>
ogbn-arxiv	ACC	0.235	<u>0.345</u>	0.336		<b>0.388</b>
	NMI	0.265	<u>0.463</u>	0.457	OOM	<b>0.469</b>
	ARI	0.227	<u>0.252</u>	0.247		<b>0.310</b>
	F1	0.089	<b>0.270</b>	0.251		<u>0.266</u>
Reddit	ACC	0.240	<u>0.832</u>	0.785		<b>0.911</b>
	NMI	0.360	<u>0.852</u>	0.836	OOM	<b>0.875</b>
	ARI	0.145	<u>0.842</u>	0.783		<b>0.907</b>
	F1	0.134	<u>0.714</u>	0.660		<b>0.853</b>
ogbn-products	ACC	0.144	<u>0.391</u>	0.387		<b>0.425</b>
	NMI	0.079	<u>0.525</u>	0.510	OOM	<b>0.551</b>
	ARI	0.059	<u>0.192</u>	0.177		<b>0.215</b>
	F1	0.035	<u>0.244</u>	0.222		<b>0.276</b>